Inorganic Chemistry

Article

pubs.acs.org/IC

Ion Exchange in Hydroxyapatite with Lanthanides

Jacqueline F. Cawthray,[†,‡] A. Louise Creagh,[§,‡] Charles A. Haynes,*[,§] and Chris Orvig*[,†]

[†]Medicinal Inorganic Chemistry Group, Department of Chemistry, University of British Columbia, 2036 Main Mall, Vancouver, British Columbia, Canada V6T 1Z1

[§]Michael Smith Laboratories and Department of Chemical and Biological Engineering, University of British Columbia, Vancouver, British Columbia, Canada V6T 1Z4

Supporting Information

ABSTRACT: Naturally occurring hydroxyapatite, $Ca_5(PO_4)_3(OH)$ (HAP), is the main inorganic component of bone matrix, with synthetic analogues finding applications in bioceramics and catalysis. An interesting and valuable property of both natural and synthetic HAP is the ability to undergo cationic and anionic substitution. The lanthanides are well-suited for substitution for the Ca^{2+} sites within HAP, because of their similarities in ionic radii, donor atom requirements, and coordination geometries. We have used isothermal titration calorimetry (ITC) to investigate the thermodynamics of ion exchange in HAP with a representative series of lanthanide ions, La^{3+}, Sm^{3+}, Gd^{3+}, Ho^{3+}, Yb^{3+} and Lu^{3+}, reporting the association constant (K_a), ion-exchange thermodynamic parameters (ΔH, ΔS, ΔG), and binding stoichiometry (n). We also probe the nature of the La^{3+}:HAP interaction by solid-state nuclear magnetic resonance (^{31}P NMR), X-ray diffraction (XRD), and inductively coupled plasma−optical emission spectroscopy (ICP-OES), in support of the ITC results.

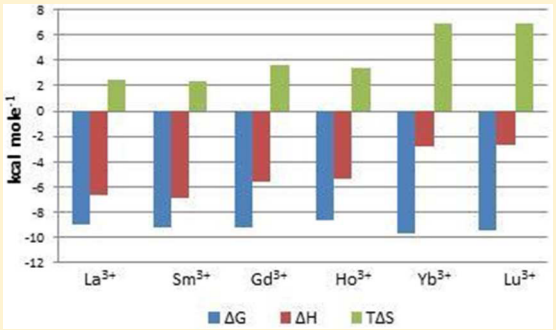

INTRODUCTION

Hydroxyapatite ($Ca_5(PO_4)_3(OH)$, HAP) is of considerable interest to many areas of science, as well as in the dental, medical, and biomaterials industries.[1] In biology, HAP is the main mineral component of bone and dental tissues. It is a porous structure that is constantly being remodeled, with the process of bone formation by osteoblasts and bone resorption by osteoclasts being tightly regulated under normal conditions. An imbalance within the remodeling process can lead to bone resorption diseases, such as osteoporosis. HAP ceramics are able to conduct new bone formation on their surface. Therefore, synthetic versions of HAP are important biomaterials for use in dental and orthopedic procedures. They share many structural and chemical similarities with biological apatite, including the same bioactivity and osteoconductivity, and have, consequently, become an important biomaterial for medical devices, implants, and tissue engineering.[2] In addition, HAP and apatites are employed as industrial catalysts,[3,4] adsorbents for removing toxic substances[5,6] and stationary-phase matrices for the chromatographic purification of proteins.[7]

Biological and synthetic HAP both crystallize in the hexagonal form, having the $P6_3/m$ space group with two formula units per cell, each with 44 atoms and a Ca/P ratio of 1.67.[8,9] There are two crystallographically distinct Ca sites in the HAP unit cell, as shown in Figure 1: Ca(1) and Ca(2). The four Ca(1) atoms are coordinated by nine O atoms belonging to six PO_4^{3-} anions, whereas the six Ca(2) ions are seven-coordinated with five PO_4^{3-} groups and the hydroxide ion.

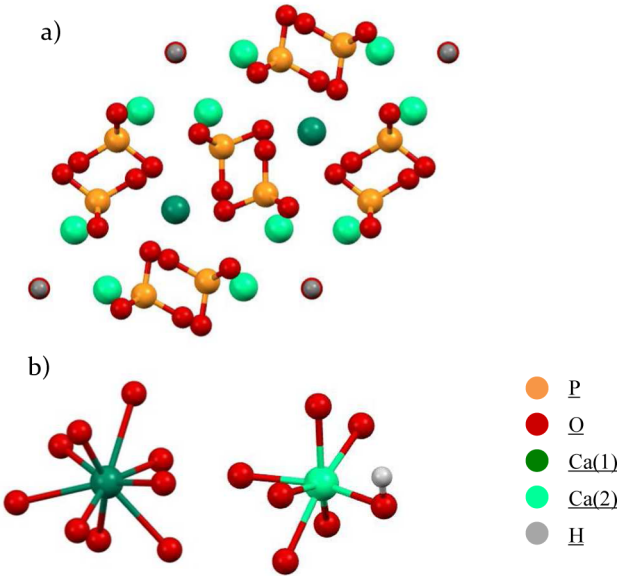

Figure 1. Calcium hydroxyapatite crystal structure: (a) as viewed along the c-axis and (b) indicating the coordination around the Ca(1) and Ca(2) centers.[24]

Received: October 6, 2014
Published: January 16, 2015

DOI: 10.1021/ic502425e
Inorg. Chem. 2015, 54, 1440−1445

Generally, the OH lies parallel to the *c*-axis and shows some disorder in the orientation in the hexagonal form of HAP.[10,11] The bonding between the PO_4^{3-} tetrahedra, the OH groups, and the Ca ions are dominated by ionic interactions, whereas predominantly covalent interactions are observed between atoms within the PO_4^{3-} groups and the O and H groups.[12] Therefore, HAP can be viewed as repeating units of PO_4 tetrahedra connected by ionic interactions with Ca and OH groups.

An important and interesting property of biological and synthetic HAP is its ability to undergo substitution of both cations (Ca^{2+}) and anions (PO_4^{3-} and/or OH^-).[2,13−16] Both Ca sites, Ca(1) and Ca(2), are available for cationic substitution with some metals showing a preference for one Ca site over the other.[17] Ion exchange of Ca^{2+} by either bivalent or trivalent ions can be expected to influence the biological, chemical, and physical properties of HAP.[18,19] For instance, in biological hydroxyapatite, magnesium and sodium are readily substituted for calcium, and the presence of magnesium in HAP improves its bioactivity, including stimulated osteoblast activity.[20,21]

Synthetic HAP doped with Zn^{2+}, In^{3+}, or Bi^{3+} was also shown to be effective at enhancing osteoblast activity, including osteoblast adhesion and osteoblast differentiation, which are important properties for coatings on orthopedic or dental implants.[23]

It is known that lanthanides—the 14 4f-block elements, plus lanthanum—have a high affinity for HAP.[25,26] The lanthanide ions, collectively designated Ln^{3+}, share similar ionic radii to Ca^{2+} ions (see Table 1), and have similar donor atom and coordination geometry preferences. The lanthanide contraction causes a decrease in the effective ionic radii with increasing atomic number, in 6-coordination, from 103.2 pm for La^{3+} to 86.1 pm for Lu^{3+}, which leads to greater charge density, compared to that of Ca^{2+} ions.[22] This higher charge density translates into a high affinity of Ln^{3+} ions for Ca^{3+} sites. In biological systems, the affinity of the radionuclide ^{153}Sm for Ca^{2+} sites in HAP is utilized for pain treatment associated with terminal bone cancer, whereas complexes of gadolinium^{3+} and terbium^{3+} are used as bone-targeting contrast agents.[27,28] They are also employed as novel scaffolds in various bone applications such as bone tissue regeneration.[23] Our interest in this field lies with the use of lanthanide ions for the treatment of bone resorption, because of its influence on the bone remodeling cycle.[29−31]

Table 1. Lanthanide Ions, and Their Ionic Radii, for a Coordination Number of 6[a]

lanthanide ion, Ln^{3+}	ionic radii (pm)	lanthanide ion, Ln^{3+}	ionic radii (pm)
Ca^{2+}	100	Gd^{3+}	93.8
La^{3+}	103.2	Tb^{3+}	92.3
Ce^{3+}	101	Dy^{3+}	91.2
Pr^{3+}	99	Ho^{3+}	90.1
Nd^{3+}	98.3	Er^{3+}	89
Pm^{3+}	97	Tm^{3+}	88.8
Sm^{3+}	95.8	Yb^{3+}	86.8
Eu^{3+}	94.7	Lu^{3+}	86.1

[a]Data taken from ref 22.

The incorporation of lanthanide ions into HAP via Ca^{2+}-ion exchange is of considerable interest, because of the control it gives over the bulk properties of HAP. However, there are few in-depth studies showing what drives ion exchange between a Ln^{3+}-ion-containing solution and HAP particles. There has been significant experimental and theoretical research done into the structural modifications induced by ion exchange in the HAP structure.[32,33] While it is known that lanthanide ions can replace calcium in the bone mineral hydroxyapatite, the strength of this exchange reaction and the factors influencing binding are not well-understood. Here, we report the direct measurement of the interaction of a series of lanthanides with HAP by isothermal titration calorimetry (ITC). ITC has been successfully used to probe the binding mechanism of bisphosphonates to HAP,[34] the binding of small proteins to HAP,[35] and the binding of metals to protein.[36−38] ITC is a suitable method for measuring ion exchange in HAP, because it is a sensitive and quantitative technique that does not require a homogeneous solution or the labeling of analytes. From the resulting data, we report, for the ion-exchange process, the equilibrium constant (K_a) and thermodynamics (ΔH, ΔS, ΔG), as well as the complex stoichiometry. We also investigate La^{3+}-ion exchange in HAP by solid-state ^{31}P NMR, X-ray diffraction (XRD), and inductively coupled plasma optical emission spectroscopy (ICP-OES), in support of the ITC results.

EXPERIMENTAL SECTION

General. High-purity water (18.2 MΩ cm, ELGA Purelab Options and ELGA Purelab Ultra) was used in all experiments. All glassware was soaked overnight in HNO_3 (5%) and thoroughly rinsed with deionized water, followed by Milli-Q water (Millipore Corp.) to remove any adventitious metal. Metal perchlorates as either the salts or 50% solutions were purchased from Alfa Aesar and used without further purification. Piperazine and hydroxyapatite were purchased from Sigma−Aldrich. All metal-ion solutions were prepared the day of use. ICP-OES measurements were performed on a Varian Model 725ES optical emission spectrometer. Standards (La, Ca, and P, 1000 $\mu g\ mL^{-1}$ in 2% HNO_3) for ICP-OES were purchased from High Purity Standards. The Ca^{2+} and PO_4^{3-} contents (Ca/P molar ratio of 1.65) for the hydroxyapatite used in this study were determined by ICP-OES. Solid-state ^{31}P NMR data were acquired on a Bruker Model Avance 400 MHz spectrometer running with XwinNMR 2.6 in a simple one-pulse experiment. The magic-angle spinning (MAS) speed was set at 6 kHz. The total number of scans was 256, with a recycle delay of 5 s. The chemical shift of ^{31}P was referenced to $NH_4H_2PO_4$. The NMR data were apodized with a 50 Hz Lorentzian broadening function and zero-filled once prior to Fourier transform. Powder XRD samples were run on a Bruker Model D8 Avance powder X-ray diffractometer in Bragg−Brentano configuration equipped with a LynxEye silicon strip detector. A copper source was used with a Ni filter to strip out the Cu Kβ radiation. The X-ray generator was set to 40 kV and 40 mA, and data were collected over the range of 5°−75° 2θ. The samples were rotated during data collection.

Isothermal Titration Calorimetry (ITC). All ITC experiments were performed on a MicroCal MCS-ITC microcalorimeter (Malvern, U.K.). Reference and sample solutions were degassed 8 min with stirring at room temperature before loading in the ITC. ITC experiments of metal-ion exchange reactions in HAP were carried out at pH 5.00 (±0.05) (100 mM piperazine buffer) and, therefore, the equilibrium constants obtained are, by definition, condition-dependent values. The reactions were analyzed in terms of Ca^{2+} for Ln^{3+} ion exchange within a formula unit of HAP in the absence of metal hydroxides that form at higher pH (e.g., see Figure S1 in the Supporting Information shows speciation of La^{3+} with pH; all La^{3+} exists as the free metal ion $[La(H_2O)_6]^{3+}$ at pH 5).[39] Titrations were performed by injecting consecutive 10-μL aliquots of a Ln^{3+}-ion solution (0.4−4 mM) into an ITC cell (volume = 1.4 mL) containing HAP (0.02−0.2 mM HAP formula unit). Control experiments (heats of dilution) were performed by titrating a Ln^{3+}-ion solution into a piperazine buffer containing no HAP. Each ITC experiment was

DOI: 10.1021/ic502425e
Inorg. Chem. 2015, 54, 1440−1445

performed on three or more independent runs. The data were fitted to a bimolecular-bimolecular exchange model to obtain a site-averaged K_a and ΔH (the enthalpy change for the exchange reaction, in kcal/mol), as well as an estimate of n (number of Ln^{3+} binding sites per HAP formula unit). Standard deviations were regressed from the cumulative results for the set of ITC runs.

Ion Exchange with Lanthanum. HAP particles were suspended in piperazine buffer pH 5.0 (100 mM) and stirred for 1 h to equilibrate. Solutions containing the appropriate amount of La^{3+} were added to the HAP suspension and stirred an additional 2 h in order to reach equilibrium for the ion exchange. The HAP particles were separated from the solution by centrifugation for 25 min and washed with buffer (three times). Samples were then freeze-dried prior to analysis via ^{31}P NMR or XRD, or digested for ICP-OES.

Acid Digestion for ICP-OES Analysis. All samples (particles, supernatants, and washes) were freeze-dried and then dissolved in 4 mL of concentrated nitric acid (Optima), transferred to test tubes and placed in a heating block with Teflon boiling chips. Samples were heated at 105 °C for 24 h prior to the addition of 4 mL of 30% hydrogen peroxide. Samples were heated a further 24 h at 140 °C and then evaporated to dryness by heating at 150 °C. For ICP-OES, samples were redissolved in 10 mL of 10% nitric acid (Optima) with europium as the internal standard. All experiments were performed in triplicate.

RESULTS

ITC experiments were used to quantify the thermodynamics of ion exchange in HAP for a representative set of metal ions ranging across the lanthanide series. Figure 2 shows a typical

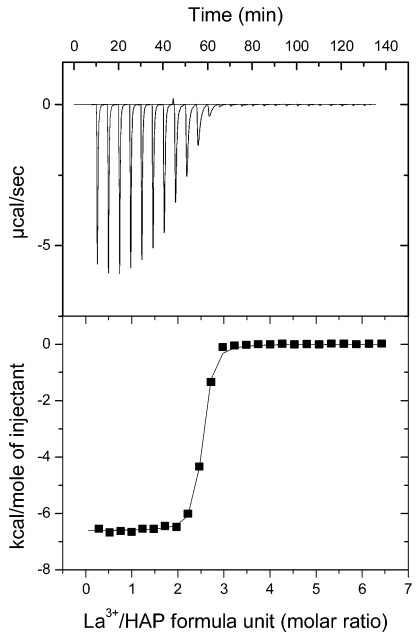

Figure 2. ITC analysis of La^{3+}-hydroxyapatite titration at 37 °C: (Top) raw titration data for 10-μL injections of 3.15 mM La^{3+} into the ITC cell containing 0.1 mM formula units of hydroxyapatite in 100 mM piperazine pH 5.0, and (bottom) integrated heat data (points) and best fit (line) to a one-site bimolecular−bimolecular binding model.

ITC titration (in this case, for La^{3+}, the largest of the lanthanide ions) into a HAP suspension at pH 5.0. ITC titrations of Sm^{3+}, Gd^{3+}, Ho^{3+}, Yb^{3+}, and Lu^{3+} into HAP are shown in Figures S2−S6 in the Supporting Information. The exchange is exothermic and rapid for molar ratios of <1.5 La^{3+}/(HAP formula unit). At molar ratios between 1.5 and 3, broader peaks are observed, indicating a slower binding event. Table 2 and Figure 3 summarize the exchange thermodynamics for all metal ions

Table 2. Summary of Ln^{3+} into Hydroxyapatite Ion-Exchange Thermodynamics at 37 °C, as Determined by ITC[a]

metal	n	K_a ($\times 10^6$)	ΔG (kcal/mol)	ΔH (kcal/mol)	$T\Delta S$ (kcal/mol)
La^{3+}	2.4(1)	2.4(2)	−9.06	−6.61(8)	2.45
Sm^{3+}	2.0(3)	3(1)	−9.1	−7.0(9)	2.2
Gd^{3+}	2.9(3)	3(1)	−9.2	−5.60(6)	3.6
Ho^{3+}	1.9(1)	1.5(7)	−8.7	−5.4(1)	3.4
Yb^{3+}	3.5(5)	6(3)	−9.5	−2.7(4)	6.9
Lu^{3+}	2.9(3)	8(4)	−9.7	−2.8(3)	6.9

[a] n represents the average number of Ln^{3+} binding sites per HAP formula unit, and ΔG, ΔH, and $T\Delta S$ values are expressed per mole of Ln^{3+} bound. The HAP formula unit is $Ca_5(PO_4)_3(OH)$.

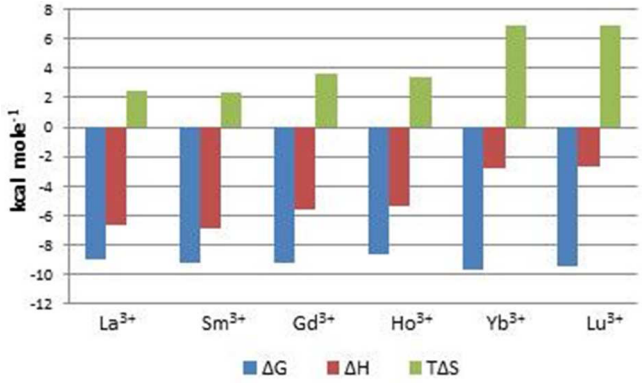

Figure 3. Thermodynamic changes (ΔG, ΔH, and $T\Delta S$) for exchange of representative ions in the lanthanide series into a formula unit of hydroxyapatite (HAP). The enthalpic contribution to the exchange reaction decreases, while the favorable entropic contribution increases as one moves across the series.

studied. Generally, 2−3 lanthanide ions exchange per formula unit of HAP. Incomplete replacement of Ca ions for La ions was observed, possibly related to the charge imbalance in the matrix that arises from the higher valence of La(III) vs Ca(II). More interestingly is the finding that the exchange of Ca^{2+} for Ln^{3+} in HAP is driven in part by entropy, which likely reflects the gain in entropy associated with proton release as Ca^{2+} is displaced by La^{3+}.

In order to determine the composition of the HAP particles following treatment with various La^{3+} concentrations, the La^{3+} and Ca^{2+} contents in the particles and solutions were analyzed by ICP-OES. Figure 4 shows the amount of La^{3+} and Ca^{2+} in the equilibrated HAP pellet (in millimoles) against the initial amount of La^{3+} in solution, given as the atomic ratio X_{metal} (= $La^{3+}/(Ca^{2+} + La^{3+})$). The amount of La^{3+} in the pellet increases as the concentration of La^{3+} increases in the initial solution, and a concomitant decrease in the amount of Ca^{2+} in the pellet is also observed. Loading of La^{3+} into HAP through displacement of Ca^{2+} increases up to an initial $La^{3+}/(Ca^{2+} + La^{3+})$ molar ratio between ca. 0.2−0.4, above which no further change in either La^{3+} or Ca^{2+} loading is observed. At this point, we see that the molar ratio of La^{3+} to HAP is ~2:1, which is consistent with the stoichiometry estimated from the ITC titration of La^{3+} into HAP.

DOI: 10.1021/ic502425e
Inorg. Chem. 2015, 54, 1440−1445

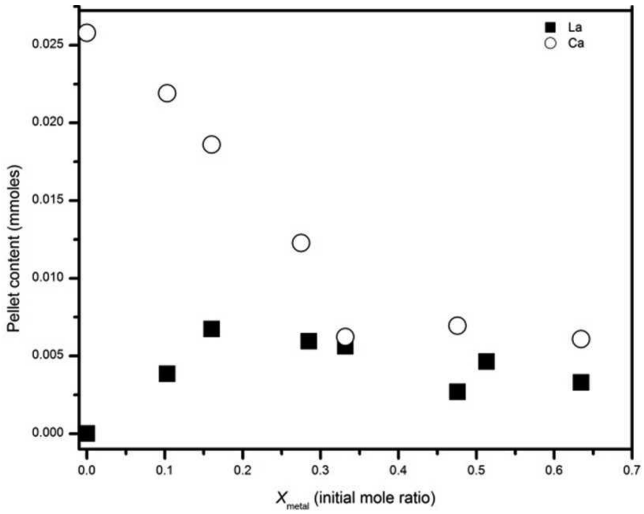

Figure 4. Amount of La^{3+} and Ca^{2+} in the HAP pellet, following the immersion of HAP particles in La^{3+} solution (pH 5, 100 mM piperazine).

Having established ion exchange between La^{3+} and the Ca^{2+} in hydroxyapatite, we used NMR to probe the effect of the exchange on the structure of HAP. The solid-state ^{31}P NMR spectrum used to characterize the structure of the HAP particles following treatment with La^{3+} solutions is shown in Figure 5. For comparison purposes, the ^{31}P NMR spectra of

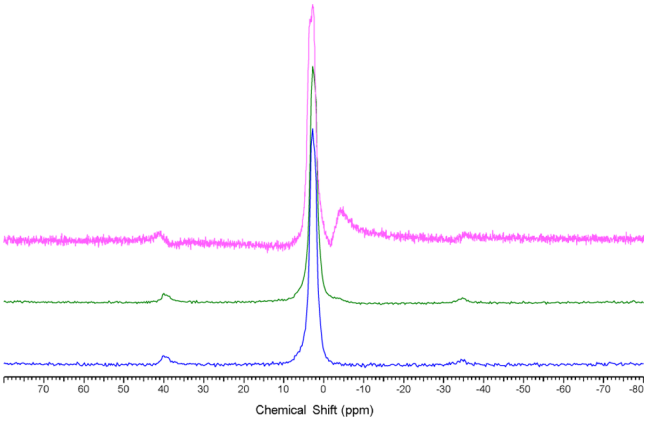

Figure 5. Comparison of the ^{31}P NMR spectra obtained for HAP (lower spectrum), HAP particles obtained from immersion of HAP in a solution containing an excess of La^{3+} (middle spectrum), and HAP mixed with $LaPO_4$ (upper spectrum).

HAP (untreated), and HAP (untreated) mixed with commercially available $LaPO_4$, are also presented. We included the $LaPO_4$ study to ensure that the reaction between the metal ion and HAP involves the incorporation of La^{3+} into HAP and not the formation of insoluble $LaPO_4$.[40] A single peak at 2.81 ppm is observed for untreated HAP (cf. 2.85 ± 0.05).[41] There is no appreciable difference in the ^{31}P NMR spectrum for HAP particles treated with a solution of an excess of La^{3+} with a single peak observed. Two peaks are observed in the ^{31}P NMR spectrum from a mixture of untreated HAP and $LaPO_4$. The first, at ~2.81 ppm, can be assigned to HAP, whereas the $LaPO_4$ peak appears at −4.38 ppm. ^{31}P NMR showed that there is no difference between the spectrum for HAP and that for HAP particles immersed in a solution containing an excess of La^{3+}. In order to verify the incorporation of lanthanides into HAP, we also performed a similar ^{31}P NMR experiment using the paramagnetic ion Yb^{3+} as a probe. The solid-state ^{31}P NMR spectrum obtained as shown in Figure S8 in the Supporting Information clearly shows that the lanthanide is incorporated into the HAP pallet.

Further evidence that a La^{3+}/Ca^{2+} ion-exchange process is occurring, and not merely dissolution of HAP accompanied by formation of insoluble $LaPO_4$, was obtained from additional ITC experiments. In Figure S7 in the Supporting Information, raw ITC titrations of either La^{3+} into HAP or La^{3+} into varying concentrations of phosphate are compared. It is clear that the two processes are not the same as those indicated by both the shape and size of the peaks.

Finally, the incorporation of La^{3+} into HAP does not significantly alter the HAP structure, as evidenced by the powder XRD patterns of untreated HAP, La^{3+}-treated HAP, and HAP mixed with $LaPO_4$ reported in Figure 6. The patterns of untreated and La^{3+}-treated HAP are characteristic of HAP and are both well-fitted to the HAP model (JCPDS File Card No. 9-432).

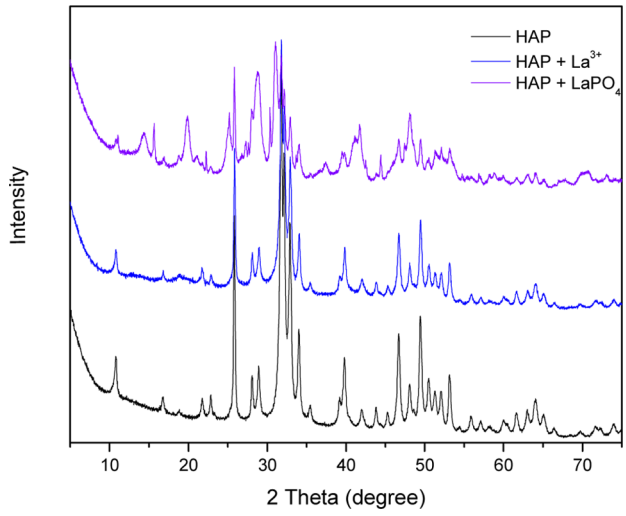

Figure 6. Powder XRD patterns obtained for HAP (lower spectrum), HAP particles obtained from immersion in a solution with an excess of La^{3+} (middle spectrum), and HAP mixed with $LaPO_4$ (upper spectrum).

DISCUSSION

Substitution of Ca^{2+} with trivalent ions requires charge balance. This can occur through either (i) the generation of vacant cation site(s) or (ii) the loss of a proton from OH^- to give an O^{2-} ion. Evidence from previous studies seems to indicate the latter is the case for synthetic La-doped HAP produced by precipitation.[42] It has also been shown that La^{3+} prefers to exchange at Ca(2) sites. Each OH^- anion has ionic interactions with Ca(2) but not Ca(1); therefore, preferred substitution at Ca(2) sites with a trivalent metal is electrostatically driven, as evidenced by short $La^{3+}\cdots O^{2-}$ interatomic distances.[43]

Some trends are observed in the thermodynamic data for the ion-exchange reaction as one moves across the lanthanide series (down Table 2) and, thus, the associated decreasing size and increasing charge density of the lanthanide ion. These trends are clearly seen in Figure 3. The binding affinity of a given lanthanide for HAP increases modestly as the ion size

DOI: 10.1021/ic502425e
Inorg. Chem. 2015, 54, 1440−1445

decreases. For larger ions in the series, the exchange reaction is largely driven by enthalpy, as expected for ion pairing, but also by a modest positive change in entropy. While both remain favorable across the series, the enthalpic contribution diminishes and $T\Delta S$ becomes dominant as the size of the lanthanide ion decreases. As noted above, the incorporation of Ln^{3+} into HAP at the Ca(2) site is accompanied by the transformation of OH^- to O^{2-}.[42] However, in our system, the freed proton is taken up by the buffer anion, and, thus, the entropy of the proton released from HAP will not change appreciably. Therefore, the observed favorable change in entropy is most likely related to differences in the solvation of calcium and lanthanide ions in water.

Lanthanide ions are kosmotropes, serving to increase the organization of solvating water molecules and increase the overall density of hydrogen bonding in solution (beyond the hydration shell of the ion).[44] This kosmotropic effect is enhanced as the lanthanide ion becomes smaller; thus, at an equivalent molar concentration, a binary aqueous solution containing a Yb^{3+}-ion salt will have a lower entropy than one containing the corresponding La^{3+}-ion salt. While Ca ions are also considered to be "structure makers", their effect on the hydrogen-bond structure is weaker than that observed for ions in the lanthanide series.[44] When a lanthanide ion displaces a Ca ion in HAP, and therefore a Ca ion replaces a lanthanide ion in solution, the net effect on the system will therefore be to increase solvent disorder, thus explaining, in part, the positive ΔS for the exchange reaction and its increasing favorability with increasing lanthanide-ion charge density. It is also consistent with the observed reduction in the favorability of ΔH for the exchange reaction. As the Ln-ion size decreases, the net change in solvent hydrogen-bond density increases in the exchange reaction, as does the $Ln^{3+}-O^{2-}$ interatomic distance.

ITC results for each Ln^{3+} metal ion show two distinct kinetic phases, with peaks in the early part of the titration rapidly returning to baseline, and a slower binding process emerging as saturation is approached. The rapid binding event is consistent with ion exchange at solvent-accessible binding sites, with the slower kinetic process likely indicative of exchange reactions involving slower ion mass transfer to and from less-accessible sites that become occupied at intermediate and higher molar ratios.

Using ICP-OES, we have established that the reaction between La^{3+} and HAP involves incorporation of the lanthanide ions into the HAP structure, as opposed to nonspecific surface interactions (Figure 4). ICP-OES, ^{31}P solid-state NMR, and powder XRD data indicate that the metal-ion exchange process does not alter the crystallinity of HAP. Moreover, solid-state ^{31}P NMR spectroscopy data clearly show that La^{3+} incorporation does not significantly alter the chemical environment of the PO_4^{3-} (see Figure 5). Previous studies have suggested that the reaction of La^{3+} with HAP leads to the dissolution of the HAP and the production of insoluble $LaPO_4$.[40,45] We have compared the solid-state ^{31}P NMR spectra of HAP, La^{3+}-treated HAP, and untreated HAP in the presence of $LaPO_4$ and do not observe evidence for the formation of $LaPO_4$ when La^{3+} is reacted with HAP. If this were the case, we would expect to see two peaks in the HAP-treated spectra; but only one peak is observed, which corresponds, in shape and chemical shift, to the single peak observed in the spectra for untreated HAP. These results were confirmed through powder XRD studies that show that the crystalline structure is not significantly altered upon the incorporation of La^{3+} into HAP. Moreover, ITC results for La^{3+} titrations into PO_4^{3-} solutions show very small exothermic peaks when compared to the titration of La^{3+} into HAP solution (see Figure S7 in the Supporting Information). Thus, we are confident that we are observing the incorporation of La^{3+} into HAP and not the formation of $LaPO_4$.

CONCLUSIONS

We have employed isothermal titration calorimetry (ITC) to study the thermodynamics of ion exchange in hydroxyapatite (HAP) with six representative metal ions from the lanthanide-(III) series. The binding constant (K_a) for the exchange of lanthanides into HAP increases as the ion size decreases and is driven, in part, by enthalpy, as expected for ion pairing, and by entropy, as expected for exchange of ions having different solvation properties in water. We have shown the interaction to involve ion exchange between the lanthanide ion and the Ca ion within the HAP. For lanthanum, the ion exchange does not significantly alter the structure of HAP, according to both powder XRD and ^{31}P solid-state NMR data.

ASSOCIATED CONTENT

Supporting Information

Lanthanum speciation plot (Figure S1) and additional ITC data (Figures S2–S7). This material is available free of charge via the Internet at http://pubs.acs.org.

AUTHOR INFORMATION

Corresponding Authors

*E-mail: israels@chbe.ubc.ca (C. A. Haynes).
*E-mail: orvig@chem.ubc.ca (C. Orvig).

Author Contributions

‡These authors contributed equally.

Author Contributions

The manuscript was written through contributions of all authors. All authors have given approval to the final version of the manuscript.

Funding

We acknowledge support from the Canadian Institutes of Health Research (CIHR) and the Natural Sciences and Engineering Research Council (NSERC) for their Collaborative Health Research Projects (CHRP) funding.

Notes

The authors declare no competing financial interest.

ACKNOWLEDGMENTS

We wish to thank the following individuals for their assistance: Dr. Zhicheng (Paul) Xia, for his assistance with NMR; Maureen Soon, for her assistance with ICP-OES; Anita Lam, for her assistance with XRD; and Yasir Makhdoom, for his assistance with ITC. C.O. acknowledges the Canada Council for the Arts for a Killam Research Fellowship (2011–2013), the University of Canterbury for a Visiting Erskine Fellowship (2013), and the Alexander von Humboldt Foundation for a Research Award, as well as Prof. Dr. Peter Comba and his research group in Heidelberg for hospitality and interesting discussions.

ABBREVIATIONS

HAP, hydroxyapatite; ICP-OES, inductively coupled plasma–optical emission spectroscopy; ITC, isothermal titration calorimetry; NMR, nuclear magnetic resonance spectroscopy;

DOI: 10.1021/ic502425e
Inorg. Chem. 2015, 54, 1440–1445

XRD, X-ray diffraction; Ca(1) and Ca(2) refer to the two crystallographically distinct Ca sites

REFERENCES

(1) Rey, C. In *Calcium Phosphates in Biological and Industrial Systems*; Amjad, Z., Ed.; Springer: Boston, MA, 1998; pp 217−251.
(2) Cho, J. S.; Yoo, D. S.; Chung, Y.-C.; Rhee, S.-H. *J. Biomed. Mater. Res., Part A* **2014**, *102*, 455.
(3) Matsumura, Y.; Moffat, J. B.; Sugiyama, S.; Hayashi, H.; Shigemoto, N.; Saitoh, K. *J. Chem. Soc. Faraday Trans.* **1994**, *90*, 2133.
(4) Mori, K.; Yamaguchi, K.; Mizugaki, T.; Ebitani, K.; Kaneda, K. *Chem. Commun.* **2001**, 461.
(5) Mavropoulos, E.; Rossi, A. M.; Costa, A. M.; Perez, C. A. C.; Moreira, J. C.; Saldanha, M. *Environ. Sci. Technol.* **2002**, *36*, 1625.
(6) Monteil-Rivera, F.; Fedoroff, M.; Jeanjean, J.; Minel, L.; Barthes, M.; Dumonceau, J. *J. Colloid Interface Sci.* **2000**, *221*, 291.
(7) Scopes, R. K. *Protein Purification: Principles and Practice*; Springer Science & Business Media: New York, 1994; p 380.
(8) Kay, M.; Young, R.; Posner, A. *Nature* **1964**, *204*, 1050.
(9) Posner, A. S.; Perloff, A.; Diorio, A. F. *Acta Crystallogr.* **1958**, *11*, 308.
(10) Elliott, J.; Wilson, R.; Dowker, S. *Adv. X-ray Anal.* **2002**, *45*, 172.
(11) De Leeuw, N. H. *Chem. Commun.* **2001**, 1646.
(12) Snyders, R.; Music, D.; Sigumonrong, D.; Schelnberger, B.; Jensen, J.; Schneider, J. M. *Appl. Phys. Lett.* **2007**, *90*, 193902.
(13) Bigi, A.; Boanini, E.; Capuccini, C.; Gazzano, M. *Inorg. Chim. Acta* **2007**, *360*, 1009.
(14) Laurencin, D.; Almora-Barrios, N.; de Leeuw, N. H.; Gervais, C.; Bonhomme, C.; Mauri, F.; Chrzanowski, W.; Knowles, J. C.; Newport, R. J.; Wong, A.; Gan, Z.; Smith, M. E. *Biomaterials* **2011**, *32*, 1826.
(15) Pizzala, H.; Caldarelli, S.; Eon, J.-G.; Rossi, A. M.; San Gil, R. A. S.; Laurencin, D.; Smith, M. E. *J. Am. Chem. Soc.* **2009**, *131*, 5145.
(16) Rintoul, L.; Wentrup-Byrne, E.; Suzuki, S.; Grøndahl, L. *J. Mater. Sci. Mater. Med.* **2007**, *18*, 1701.
(17) Bigi, A.; Gandolfi, M.; Gazzano, M.; Ripamonti, A.; Roveri, N.; Thomas, S. A. *J. Chem. Soc. Dalton Trans.* **1991**, 2883.
(18) Morais, D. S; Coelho, J.; Ferraz, M. P.; Gomes, P. S.; Fernandes, M. H.; Hussain, N. S.; Santos, J. D.; Lopes, M. A. *J. Mater. Chem. B* **2014**, *2*, 5872.
(19) Webster, T. J.; Ergun, C.; Doremus, R. H.; Bizios, R. *J. Biomed. Mater. Res.* **2002**, *59*, 312.
(20) Bigi, A.; Foresti, E.; Ripamonti, A.; Compostella, L.; Fichera, A. M.; Gazzano, M.; Roveri, N. *J. Inorg. Biochem.* **1988**, *34*, 75.
(21) Landi, E.; Logroscino, G.; Proietti, L.; Tampieri, A.; Sandri, M.; Sprio, S. *J. Mater. Sci. Mater. Med.* **2008**, *19*, 239.
(22) Shannon, R. D. *Acta Crystallogr., Sect. A: Cryst. Phys., Diffr., Theor. Gen. Crystallogr.* **1976**, *32*, 751.
(23) Webster, T. J.; Massa-Schlueter, E. A.; Smith, J. L.; Slamovich, E. B. *Biomaterials* **2004**, *25*, 2111.
(24) Hughes, J. M.; Cameron, M.; Crowley, K. D. *Am. Mineral.* **1989**, *74*, 870.
(25) Vidaud, C.; Bourgeois, D.; Meyer, D. *Chem. Res. Toxicol.* **2012**, *25*, 1161.
(26) Ardanova, L. I.; Get'man, E. I.; Loboda, S. N.; Prisedsky, V. V.; Tkachenko, T. V.; Marchenko, V. I.; Antonovich, V. P.; Chivireva, N. A.; Chebishev, K. A.; Lyashenko, A. S. *Inorg. Chem.* **2010**, *49*, 10687.
(27) Volkert, W. A.; Hoffman, T. J. *Chem. Rev.* **1999**, *99*, 2269.
(28) Kubícek, V.; Rudovský, J.; Kotek, J.; Hermann, P.; Vander Elst, L.; Muller, R. N.; Kolar, Z. I.; Wolterbeek, H. T.; Peters, J. A.; Lukes, I. *J. Am. Chem. Soc.* **2005**, *127*, 16477.
(29) Barta, C. A.; Sachs-Barrable, K.; Jia, J.; Thompson, K. H.; Wasan, K. M.; Orvig, C. *Dalton Trans.* **2007**, 5019.
(30) Mawani, Y.; Cawthray, J. F.; Chang, S.; Sachs-Barrable, K.; Weekes, D. M.; Wasan, K. M.; Orvig, C. *Dalton Trans.* **2013**, *42*, 5999.
(31) Von Rosenberg, S. J.; Wehr, U. A. *J. Anim. Physiol. Anim. Nutr.* **2012**, *96*, 885.
(32) Terra, J.; Gonzalez, G. B.; Rossi, A. M.; Eon, J. G.; Ellis, D. E. *Phys. Chem. Chem. Phys.* **2010**, *12*, 15490.
(33) Mayer, I.; Layani, J. D.; Givan, A.; Gaft, M.; Blanc, P. *J. Inorg. Biochem.* **1999**, *73*, 221.
(34) Mukherjee, S.; Huang, C.; Guerra, F.; Wang, K.; Oldfield, E. *J. Am. Chem. Soc.* **2009**, *131*, 8374.
(35) Goobes, R.; Goobes, G.; Campbell, C. T.; Stayton, P. S. *Biochemistry* **2006**, *45*, 5576.
(36) Bekker, E. G.; Creagh, A. L.; Sanaie, N.; Yumoto, F.; Lau, G. H. Y.; Tanokura, M.; Haynes, C. A.; Murphy, M. E. P. *Biochemistry* **2004**, *43*, 9195.
(37) Creagh, A. L.; Tiong, J. W. C.; Tian, M. M.; Haynes, C. A.; Jefferies, W. A. *J. Biol. Chem.* **2005**, *280*, 15735.
(38) Wilcox, D. E. *Inorg. Chim. Acta* **2008**, *361*, 857.
(39) Baes, C. F.; Mesmer, R. E. *The Hydrolysis of Cations*; Wiley: New York, 1976.
(40) Schaad, P.; Gramain, P.; Gorce, F.; Voegel, J. C. *J. Chem. Soc. Faraday Trans.* **1994**, *90*, 3405.
(41) Isobe, T.; Nakamura, S.; Nemoto, R.; Senna, M.; Sfihi, H. *J. Phys. Chem. B* **2002**, *106*, 5169.
(42) Serret, A.; Cabañas, M. V.; Vallet-Regí, M. *Chem. Mater.* **2000**, *12*, 3836.
(43) Schroeder, L. W.; Mathew, M. *J. Solid State Chem.* **1978**, *26*, 383.
(44) Marcus, Y. *Chem. Rev.* **2009**, *109*, 1346.
(45) Tanizawa, Y.; Sawamura, K.; Suzuki, T. *J. Chem. Soc. Faraday Trans.* **1990**, *86*, 4025.

DOI: 10.1021/ic502425e
Inorg. Chem. 2015, 54, 1440−1445